Mon. Not. R. Astron. Soc. **000**, 1–12 (2014) Printed 8 August 2018 (MN LATEX style file v2.2)

Inter-comparison of Radio-Loudness Criteria for Type 1 AGNs in the XMM-COSMOS Survey

Heng Hao[1,2⋆], Mark T. Sargent[3,4,5], Martin Elvis[2], Eva Schinnerer[5], Gianni Zamorani[6], Luis C. Ho[7,8,9], Jennifer L. Donley[10], Francesca Civano[2,11,12], Vernesa Smolčić[13], Annalisa Celotti[1,14,15], Joanna Kuraszkiewicz[2], Mara Salvato[16,17], Marcella Brusa[6,18,19], Peter Capak[20], Chris L. Carilli[21], Andrea Comastri[6], Chris D. Impey[22], Knud Jahnke[5], Anton M. Koekemoer[23], Kevin Schawinski[24], Jonathan R. Trump[25], C. Megan Urry[11], Cristian Vignali[6,18], Min Yun[26]

[1] *SISSA, Via Bonomea 265, I-34136 Trieste, Italy*
[2] *Harvard-Smithsonian Center for Astrophysics, 60 Garden Street, Cambridge, MA 02138, USA*
[3] *Astronomy Center, Department of Physics and Astronomy, University of Sussex, Brighton BN1 9QH, UK*
[4] *CEA-Saclay, Service d'Astrophysique, Orme des Merisiers, Bat. 709, 91191 Gif-sur-Yvette, France*
[5] *Max-Planck-Institut für Astronomie, Königstuhl 17, Heidelberg, D-69117, Germany*
[6] *INAF - Osservatorio Astronomico di Bologna, via Ranzani 1, I-40127 Bologna, Italy*
[7] *Kavli Institute for Astronomy and Astrophysics, Peking University, Beijing 100871, China*
[8] *Department of Astronomy, Peking University, Beijing, China*
[9] *The Observatories of the Carnegie Institute for Science, Santa Barbara Street, Pasadena, CA 91101, USA*
[10] *Los Alamos National Laboratory, Los Alamos, NM 87544, USA*
[11] *Yale Center for Astronomy and Astrophysics, 260 Whitney ave, New Haven, CT 06520, USA*
[12] *Dartmouth College, Department of Physics and Astronomy, 6127 Wilder Lab, Hanover, NH 03755*
[13] *Physics Department, University of Zagreb, Bijenička cesta 32, 10002 Zagreb, Croatia*
[14] *INAF - Osservatorio Astronomico di Brera, via E. Bianchi 46, I-23807 Merate, Italy*
[15] *INFN - Sezione di Trieste, via Valerio 2, 34127, Trieste, Italy*
[16] *IPP - Max-Planck-Institute for Plasma Physics, Boltzmann Strasse 2, D-85748, Garching bei München, Germany*
[17] *Excellence Cluster, Boltzmann Strasse 2, D-85748, Garching bei München, Germany*
[18] *Dipartimento di Fisica e Astronomia, Università degli studi di Bologna, viale Berti Pichat 6/2 40127 Bologna, Italy*
[19] *Max Planck Institute für Extraterrestrische Physik, Postfach 1312, 85741, Garching bei München, Germany*
[20] *Spitzer Science Center, MS 314-6, California Institute of Technology, Pasadena, CA 91125, USA*
[21] *National Radio Astronomy Observatory, P.O. Box 0, Socorro, NM 87801, USA*
[22] *Steward Observatory, University of Arizona, 933 North Cherry Avenue, Tucson, AZ 85721, USA*
[23] *Space Telescope Science Institute, 3700 San Martin Drive, Baltimore, MD 21218, USA*
[24] *Institute for Astronomy, Department of Physics, ETH Zurich,Wolfgang-Pauli-Strasse 16, CH-8093 Zurich, Switzerland*
[25] *Department of Astronomy and Astrophysics, Pennsylvania State University, University Park, PA 16802, USA*
[26] *Department of Astronomy, University of Massachusetts, Amherst, MA 01003, USA*

Version Jun 1st, 2014.

ABSTRACT

Limited studies have been performed on the radio-loud fraction in X-ray selected type 1 AGN samples. The consistency between various radio-loudness definitions also needs to be checked. We measure the radio-loudness of the 407 type 1 AGNs in the XMM-COSMOS quasar sample using nine criteria from the literature (six defined in the rest-frame and three defined in the observed frame): $R_L = \log(L_{5GHz}/L_B)$, $q_{24} = \log(L_{24\mu m}/L_{1.4GHz})$, $R_{uv} = \log(L_{5GHz}/L_{2500\mathring{A}})$, $R_i = \log(L_{1.4GHz}/L_i)$, $R_X = \log(\nu L_\nu(5GHz)/L_X)$, $P_{5GHz} = \log(P_{5GHz}(W/Hz/Sr))$, $R_{L,obs} = \log(f_{1.4GHz}/f_B)$ (observed frame), $R_{i,obs} = \log(f_{1.4GHz}/f_i)$ (observed frame), and $q_{24,obs} = \log(f_{24\mu m}/f_{1.4GHz})$ (observed frame). Using any single criterion defined in the rest-frame, we find a low radio-loud fraction of $\lesssim$5% in the XMM-COSMOS type 1 AGN sample, except for R_{uv}. Requiring that any two criteria agree reduces the radio-loud fraction to $\lesssim 2\%$ for about 3/4 of the cases. The low radio-loud fraction cannot be simply explained by the contribution of the host galaxy luminosity and reddening. The $P_{5GHz} = \log(P_{5GHz}(W/Hz/Sr))$ gives the smallest radio-loud fraction. Two of the three radio-loud fractions from the criteria defined in the observed frame without k-correction ($R_{L,obs}$ and $R_{i,obs}$) are much larger than the radio-loud fractions from other criteria.

Key words: galaxies: evolution; quasars: general; surveys

1 INTRODUCTION

Quasars are often classified into radio-loud (RL) and radio-quiet (RQ), based on the presence or absence of strong radio emission. Radio-loud quasars are generally some three orders of magnitude more powerful at GHz radio frequencies relative to their optical or infrared fluxes than RQ quasars, while in the rest of their spectral energy distributions (SEDs), from mid-infrared to X-ray, there are only subtle differences between them (e.g., Elvis et al., 1994, E94 hereinafter). The strong radio emission is a result of RL quasars having a relativistic jet that generates synchrotron radiation in the radio (see review by Harris & Krawczynski 2006).

However, even RQ quasars can be detected as radio sources (Kellermann et al. 1989). This has led to two opposing views of the radio-loudness distribution which have long been debated. The first is that the radio-loudness distribution is bimodal (e.g. Kellermann et al. 1989; Miller et al. 1990; Visnovsky et al. 1992; Ivezić et al. 2002). The other is that the distribution is continuous with no clear dividing line (Cirasuolo et al. 2003).

Typically, ∼10% of all quasars in optically selected samples are RL (e.g. Kellermann et al. 1989; Urry & Padovani 1995; Ivezić et al. 2002). Here we examine the RL fraction of the 413 type 1 AGNs in the XMM-COSMOS sample to check both the RL fraction in X-ray selected samples and the consistency among various radio-loudness criteria. In this paper, we adopt the WMAP 5-year cosmology (Komatsu et al., 2009), with H_0 =71 km s^{-1} Mpc^{-1}, $\Omega_M = 0.26$ and Ω_Λ= 0.74.

2 COSMOS TYPE 1 AGN PHOTOMETRY

The XMM-COSMOS survey (Hasinger et al. 2007) detected 1848 point sources down to $\sim 10^{-15}$ erg cm^{-2}s^{-1}. Using a likelihood ratio technique, Brusa et al (2007, 2010) identified unique counterparts of 1577 (85%) XMM-COSMOS sources in the optical photometric catalog (Capak et al. 2007). A total of 886 XMM-COSMOS sources (∼50%) have well-determined spectroscopic redshifts from optical spectra (Trump et al. 2009a, Schneider et al. 2007, Lilly et al. 2007, 2009). From these spectra, 413 are identified as type 1 AGN, with emission line FWHM> 2000 km s^{-1}, forming the XMM-COSMOS type 1 AGN sample (XC413, Elvis et al. 2012, hereafter Paper I). The XC413 sample has 43 photometry bands extending from radio to X-ray, and spans a large redshift range ($0.1 \leqslant z \leqslant 4.3$, with median 1.6), as well as both large apparent magnitude ($16.8 \leqslant i_{AB} \leqslant 25.0$ with median 21.2) and intrinsic luminosity ($44.3 \leqslant \log L_{bol} \leqslant 47.4$ with median 45.7) ranges. We now briefly review the optical, infrared (IR) and radio flux measurements which are crucial to the analysis.

All 413 quasars in XC413 have B band and J band detections (Paper I). In the mid-infrared range, 385 detections were obtained in the S-COSMOS MIPS 24μm imaging (Sanders et al. 2007; Le Floc'h et al. 2009) by searching for counterparts within 2″ of the optical counterpart. With the exception of one source (located outside the 24μm survey area), we derived 3σ upper flux density limits (∼54μJy on average) for the remaining 27 unmatched quasars using a coverage-based rms map.

In the radio, the VLA-COSMOS 1.4 GHz survey detected 2865 sources at S/N=5 (rms=8-12 μJy, depending on the position in the field; Schinnerer et al. 2010). Radio counterparts to the XMM X-ray sources were determined by cross-correlating the optical quasar positions to source positions in the VLA-COSMOS joint catalog (Schinnerer et al. 2010) within a radius of 1″. This resulted in 61 (15% of 413) successful matches with the XC413 sample.

For the unmatched XMM-COSMOS quasars, the AIPS/MAXFIT peak finding algorithm was used to search for additional radio detections within a 2.5″×2.5″ box centered on the optical coordinates. The box size is chosen because the resolution of the radio beam is 2.5″. This yielded 78 additional detections in the 3σ-5σ range. In all, we have 139 sources with larger than 3σ radio detection. We computed their total flux assuming that they are unresolved at 1.4GHz (beam FWHM 2.5″). For lower significance peaks (286 out of 413) we adopted 3σ upper flux density limits based on the local rms noise (calculated within a 17.5″×17.5″ box) at the position of the radio source. This box size was chosen based on the tests we made to obtain the most accurate map for the VLA-COSMOS Deep Project mosaic.

In summary, out of the 413 XMM-COSMOS quasars, 407 have either $> 3\sigma$ VLA detections or upper limits. We have no radio flux information about the remaining 6 AGNs as they lie outside the VLA-COSMOS 1.4 GHz coverage area, and in one case also outside the MIPS-COSMOS 24μm coverage area. We will only discuss the radio loudness for these 407 type 1 AGNs (XC407 sample) in this paper.

3 RADIO-LOUDNESS DEFINITIONS

Several criteria have been used to classify quasars as RL or RQ. As noted, mere radio detection is not enough. Radio power, either alone or relative to some other band is typically used. We determined the radio-loudness of the XC407 for nine definitions currently in use in the literature:

(i) R_L: the luminosity ratio of radio to optical emission $R_L = \log(L_{5GHz}/L_B)$ (Wilkes & Elvis 1987, Kellermann et al. 1989), with $R_L >1$ defining a RL source. This logarithmic (base ten, as for all following definitions) radio-to-optical luminosity ratio is the most widespread criterion for RL. COSMOS does not have 5 GHz coverage, but, as most of the sample sources are at redshift 1–2 (Paper I), the observed 1.4 GHz VLA band is close to the emitted 5 GHz frequency. We converted the observed 1.4 GHz luminosity to a rest-frame 5 GHz luminosity by assuming $f_\nu \propto \nu^{-0.5}$ (e.g., Ivezić 2004). For most of the quasars in the XC407 sample at redshift $z \sim 2$, the observed 1.4 GHz is at rest-frame ∼ 4.2 GHz, the residual k-correction is only 9%. The B band luminosity is the luminosity at rest-frame B band ($\lambda_{eff} = 4483\AA$) retrieved from the rest-frame SED for each quasar, that is the linear interpolation of the adjacent observed photometry after moving to the rest-frame.

(ii) $R_{L,obs}$: We also calculated $R_{L,obs} = \log(f_{1.4GHz}/f_B)$ in the observed frame without k-correction for comparison, with $R_{L,obs} > 1$ defined as radio-loud. This criteria is typically used when redshift information is not available.

As most of the XMM-COSMOS AGNs lie at redshift 1–2,

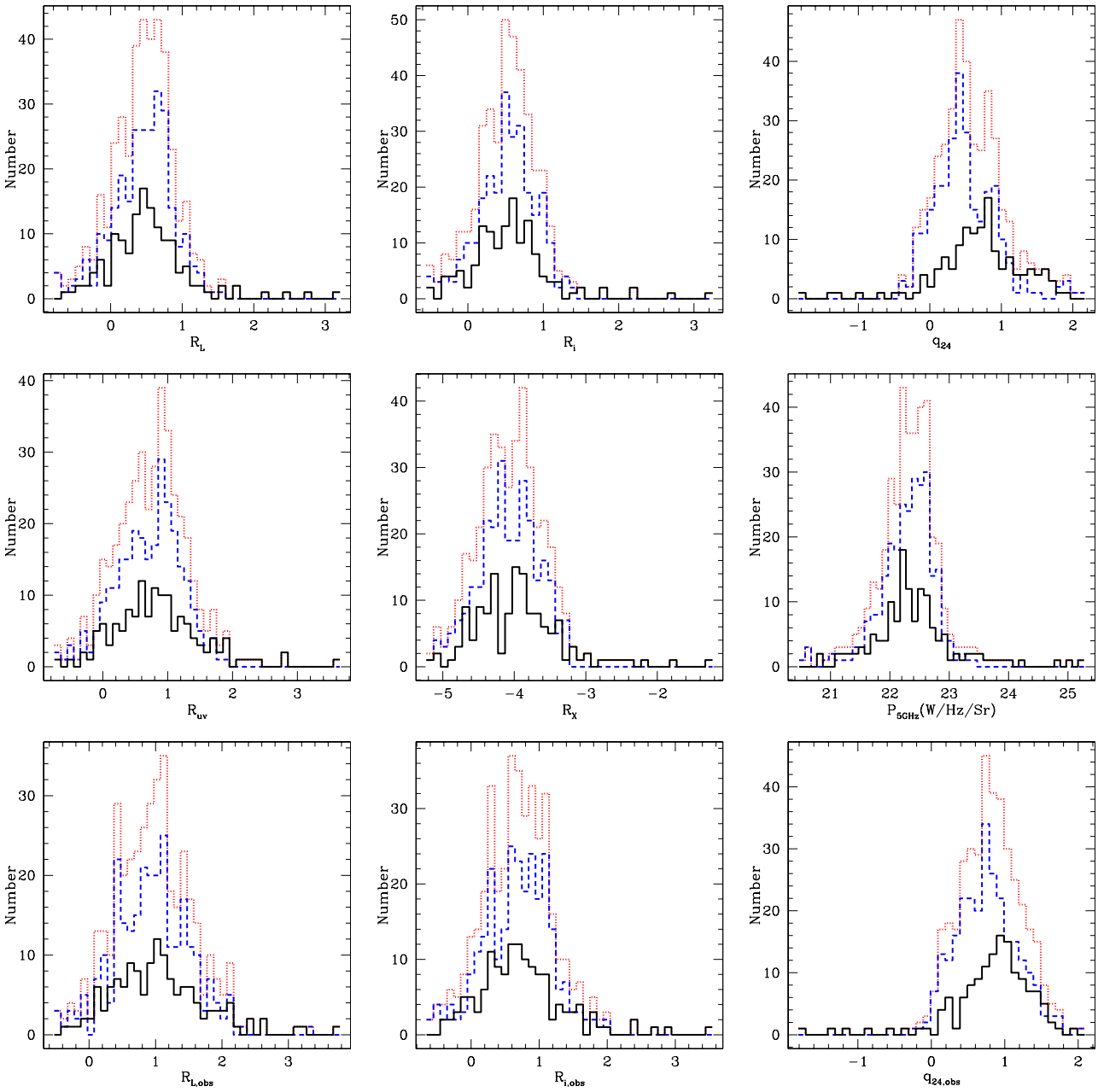

Figure 1. Distribution of radio-loudness measures: R_L, R_i, q_{24}, R_{uv}, R_X, P_{5GHz}, $R_{L,obs}$, $R_{i,obs}$, and $q_{24,obs}$. The black solid line show the distribution for quasars with radio detections; the blue dashed line show the distribution for quasars with upper limits in radio; the red dotted line show the distribution for all the 407 quasars with radio detection or upper limits.

the 1.4 GHz band lies close to rest-frame 5 GHz and the J-band lies close to rest-frame B band. Hence, for a consistency check, we can adopt $R_J = \log(f_{1.4GHz}/f_J)$ in the observed frame as an alternative definition to RL that does not involve any assumptions about the k-correction.

(iii) R_i: Balokovi$\acute{c}$ et al. (2012) defined the radio-loudness as the radio to i band luminosity ratio: $R_i = \log(L_{5GHz}/L_i)$. Here we calculate R_i using the same k-correction in the radio as in R_L and retrieve the rest-frame i band ($\lambda_{eff} = 7523\mathring{A}$) luminosity from the rest-frame SED by interpolation. We define $R_i > 1$ as radio-loud.

(iv) $R_{i,obs}$: Ivezi$\acute{c}$ et al. (2002) defined the radio-loudness as $R_{i,obs} = \log(f_{1.4GHz}/f_i)$ in the observed frame without k-correction and $R_{i,obs} > 1$ was defined as radio-loud. Considering most of the XMM-COSMOS AGNs lie at redshift 1–2, the 1.4 GHz band lies close to rest-frame 5 GHz and the K-band lies close to rest-frame i band. Similarly, we can adopt $R_K = \log(f_{1.4GHz}/f_K)$ in the observed frame without k-correction as an alternative definition to radio-loudness.

(v) q_{24}: Appleton et al. (2004) introduced a new definition of radio-loudness using the Spitzer/MIPS 24 μm flux: q_{24} = $\log(L_{24\mu m}/L_{1.4GHz})$, with $q_{24} < 0$ defined as RL. We calculated q_{24} in the rest-frame assuming the same power law in the radio as for the R_L definition and the rest frame

24μm retrieved from the rest-frame SED of each quasar. Kuraszkiewicz et al. (in preparation) studied the correlation between q_{24} and R_L for a sample with limited reddening or host contamination, and find that, on average, $R_L > 1$ corresponds to $q_{24} < 0.24$, rather than $q_{24} < 0$. We use $q_{24,K}$ to represent the criterion using this alternative dividing line.

(vi) $q_{24,obs}$: For easy comparison with $R_{L,obs}$, which is defined in the observed frame, we also check q_{24} in the observed frame and define it as $q_{24,obs} = \log(f_{24\mu m}/f_{1.4GHz})$.

Out of the 407 quasars, 25 have upper flux density limits both at 1.4 GHz and 24 μm. For these sources, q_{24} and $q_{24,obs}$ cannot be determined and we thus excluded these 25 sources from the discussion of the results for q_{24} and $q_{24,obs}$.

(vii) R_{uv}: Stocke et al. (1992) used the ratio between the 2500Å UV luminosity and radio luminosity: $R_{uv} = \log(L_{5GHz}/L_{2500\mathring{A}})$ (see also Jiang et al. 2007). This criterion has the advantage of using the peak of the SED to define radio-loudness, but is strongly affected even by modest reddening. For example, $E(B-V) > 0.3$ decreases the 2500Å UV luminosity by a factor > 7. The effect is to make more objects appear RL in X-ray selected samples, such as the XC407 sample, as these include a large number of sources with significant optical reddening compared to optically-selected samples (Paper I, Hao et al. 2013, 2014). This criterion is therefore less useful for X-ray selected samples. In the *Einstein* Extended Medium Sensitivity Survey (EMSS), radio-loudness is defined with $\alpha_{ro} = R_{uv}/5.38$ (Della Ceca et al. 1994, Zamorani et al. 1981). Sources with $\alpha_{ro} > 0.35$ are defined as RL, that is equivalent to $R_{uv} > 1.88$. We use $R_{uv,D}$ to represent the criterion.

(viii) R_X: Terashima & Wilson (2003) proposed a criterion based on the ratio between luminosity at 5 GHz and X-ray luminosity in the $2-10$ keV band. Sources with $R_X = \log(\nu L_\nu(5GHz)/L_X) > -3$ are RL (Pierce et al. 2011). This criterion is working both for heavily obscured AGN, $N_H \lesssim 10^{23} cm^{-2}$ and of being free of host galaxy contamination.

(ix) P_{5GHz}: Goldschmidt et al. (1999) proposed a criterion based solely on radio power, where sources with $P_{5GHz} = \log[P_{5GHz}(W/Hz/Sr)] > 24$ are considered to be RL. Given that Goldschmidt et al. (1999) assume a Hubble parameter H_0=50 km s^{-1} Mpc^{-1}, this criterion corresponds to $P_{5GHz} = \log[P_{5GHz}(W/Hz/Sr)] > 23.7$ for the cosmology used in this paper.

The distributions of the nine radio loudness measures are shown in Figure 1. From these plots we could only see continuous distributions with long tail on the radio loud side and there is no clear sign of bimodality. The size of the sample is still too small to give statistical significant check on the bimodality of the radio loudness measures.

4 RADIO-LOUD FRACTION

4.1 Single Criterion

The numbers and fractions of RL quasars in the sample using the nine different RL selection criteria are summarized in Table 1. The RL-fraction is calculated (a) using Kaplan-Meier product limit estimator (Kaplan & Meier 1958) if the sample is singly-censored or (b) following the iterative procedure in Schmitt (1985) if both upper and lower limits on the loudness diagnostic are present (q_{24} and $q_{24,obs}$). We also list the number of ambiguous sources in the table, which are those with upper/lower limits lying in the RL region.

Table 1. Radio-Loud Quasars by Different Criteria

criterion	N(RL)	N(RQ)	N(amb)*	Fraction(RL)
$R_L > 1$	18	367	22	$4.50\%^{+2.73\%}_{-1.52\%}$
$R_i > 1$	16	364	27	$3.98\%^{+2.67\%}_{-1.38\%}$
$q_{24} < 0$	13^a	357	12	$3.43\%^{+1.67\%}_{-1.11\%}$
$q_{24,K} < 0.24$	25^a	307	50	$7.22\%^{+2.43\%}_{-2.70\%}$
$R_{uv} > 1$	45	283	79	$11.75\%^{+4.02\%}_{-2.60\%}$
$R_{uv,D} > 1.88$	9	398	0	$2.21\%^{+2.09\%}_{-1.00\%}$
$R_X > -3$	10	397	0	$2.46\%^{+1.88\%}_{-1.23\%}$
$P_{5GHz} > 23.7$	8	399	0	$1.97\%^{+1.83\%}_{-1.03\%}$
$R_{L,obs} > 1$	67	220	120	$19.23\%^{+4.92\%}_{-3.58\%}$
$R_J > 1$	16	360	31	$4.02\%^{+2.71\%}_{-1.39\%}$
$R_{i,obs} > 1$	38	300	69	$10.03\%^{+3.79\%}_{-2.43\%}$
$R_K > 1$	10	392	5	$2.46\%^{+2.23\%}_{-1.04\%}$
$q_{24,obs} < 0$	8	370	4^b	$2.55\%^{+1.49\%}_{-1.06\%}$

*Number of ambiguous sources that with upper/lower limits in the radio-loud region. See § 4 for details.

[a,b]The 2 sources (XMM ID: 320 and 5315) with VLA detection and MIPS upper limits have upper limits on q_{24} and $q_{24,obs}$. Therefore: (a) they are already located in the RL region with upper limits, so they are RL by the q_{24} criterion; (b) they are located in the RQ region with upper limits, so they can still be RL, so they are ambiguous for the $q_{24,obs}$ criterion.

The fraction of radio-loud quasars spans a wide range from $\sim 2\%$ to $\sim 20\%$.

For the criteria defined in the rest-frame, R_{uv} classifies the largest number ($\sim 12\%$) of COSMOS AGNs as RL, where most of these quasars are RQ by all other criteria defined in the rest frame. The SEDs of the quasars classified as RL by R_{uv} but not the other criteria generally do not show a 'big blue bump' feature in their SEDs that is characteristic of unobscured quasars (Paper I). We plot the sources which have either a direct measurement or upper limit of R_{uv} that exceeds the selection threshold for radio loudness ($R_{uv} = 1$), but which are RQ according to all alternative definitions defined in the rest-frame, in the Hao et al. (2013) mixing diagram (Figure 2). These quasars are mainly located in the high reddening ($E(B-V) > 0.2$) or high galaxy fraction ($f_g > 0.4$) regions and well away from the E94 SED region (red circle in Figure 2). This suggests that they are mostly reddened or galaxy dominated sources and their apparent radio-loudness by R_{uv} is due to these contaminating factors. Note that if we change the RQ and RL dividing line, i.e. if we use the $R_{uv,D}$ criterion instead, the number of ambiguous sources would be much lower and the radio-loud fraction will drop to $\sim 2\%$. This criterion is more appropriate for X-ray selected samples.

Table 2. Radio-Loud Quasars with Two Criteria

criterion	N(RL)	N(RQ)	N(amb)*			Fraction(RL)
			1	2		
$R_L > 1$ $q_{24} < 0$	8	339	10 5^a	8 8	4	2.1%
$R_L > 1$ $R_{uv} > 1(1.88)^{**}$	18(8)	283(366)	0(10) 27(1)	0(22) 57(0)	22(0)	4.4%(2.0%)
$R_L > 1$ $R_i > 1$	14	355	4 2	5 10	17	3.4%
$R_L > 1$ $R_X > -3$	7	364	11 3	22 0	0	1.7%
$R_L > 1$ $P_{5GHz} > 23.7$	6	365	12 2	22 0	0	1.5%
$q_{24} < 0$ $R_{uv} > 1(1.88)^{**}$	$13^b(7)$	270(355)	$0(6^a)$ 32(2)	5(12) 55(0)	7(0)	3.4%(1.8%)
$q_{24} < 0$ $R_i > 1$	8	342	5^a 8	7 7	5	2.1%
$q_{24} < 0$ $R_X > -3$	7	354	6^a 3	12 0	0	1.8%
$q_{24} < 0$ $P_{5GHz} > 23.7$	6	355	7^a 2	12 0	0	1.6%
$R_{uv} > 1(1.88)^{**}$ $R_i > 1$	15(7)	277(362)	30(2) 1(9)	57(0) 5(27)	22(0)	3.7%(1.7%)
$R_{uv} > 1(1.88)^{**}$ $R_X > -3$	8(6)	281(394)	37(3) 2(4)	79(0) 0(0)	0(0)	2.0%(1.5%)
$R_{uv} > 1(1.88)^{**}$ $P_{5GHz} > 23.7$	6(5)	281(395)	39(4) 2(3)	79(0) 0(0)	0(0)	1.5%(1.2%)
$R_i > 1$ $R_X > -3$	9	363	7 1	27 0	0	2.2%
$R_i > 1$ $P_{5GHz} > 23.7$	6	362	10 2	27 0	0	1.5%
$R_X > -3$ $P_{5GHz} > 23.7$	7	396	3 1	0 0	0	1.7%
$R_{L,obs} > 1$ $q_{24,obs} < 0$	8	218	57 0	95 2^c	2	2.1%
$R_{i,obs} > 1$ $q_{24,obs} < 0$	8	293	28 0	49 2^c	2	2.1%
$R_{L,obs} > 1$ $R_{i,obs} < 0$	38	220	29 0	51 0	69	9.3%

*Number of ambiguous sources: 1) they are RL with one criterion, but RQ with the other; 2) the upper/lower limits locate in the radio-loud region for one or both criteria, that they could be RQ. See § 4 for details.

** The numbers in the parenthesis are for the $R_{uv,D}$ criterion.

^{a,b,c}The 2 sources (XMM ID: 320 and 5315) with VLA detection and MIPS upper limits have upper limits on q_{24} and $q_{24,obs}$. Therefore: (a) they are already located in the RL region with upper limits, so they are RL by the q_{24} criterion. But they are not RL in the other criterion, so they are still ambiguous sources; (b) they are already located in the RL region with upper limits, so they are RL by the q_{24} criterion. And they are RL by the R_{uv} criterion, so they are not ambiguous sources; (c) they are located in the RQ region with the upper limits, so they can still be RL, so they are ambiguous for the $q_{24,obs}$ criterion.

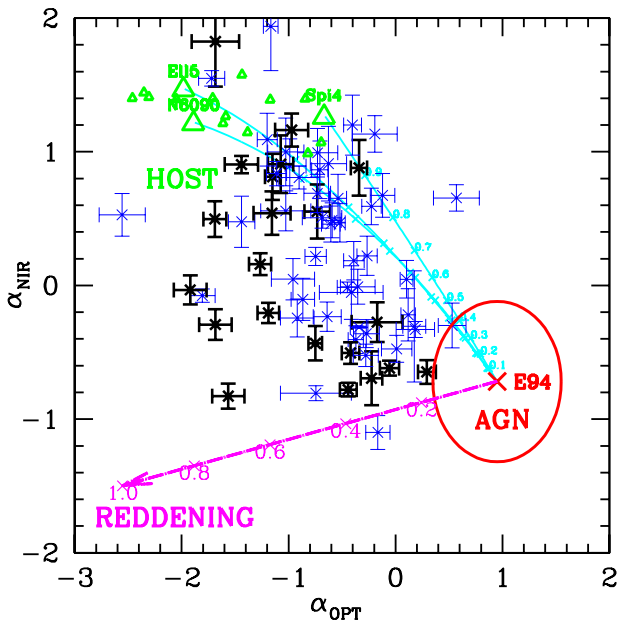

Figure 2. Mixing diagram (Hao et al. 2012) for RL quasars according to the R_{uv} criterion, but classified as RQ by all other selections. Black points are used for quasars with radio detections, blue points for "ambiguous" quasars (upper limit on R_{uv} exceeding threshold R_{uv}=1). The mixing diagram is the plot of the SED slopes α_{NIR} ($3\mu m$ to $1\mu m$) versus α_{OPT} ($1\mu m$ to $0.3\mu m$). The E94 RQ mean SED is shown as the red cross. The red circle shows the dispersion of E94. The green triangles show galaxy templates from the SWIRE template library (Polletta et al. 2007). The purple arrow represents the reddening vector for the E94 RQ mean SED. The cyan lines connect the galaxy templates and the E94 mean SED are mixing curves showing templates with different galaxy fractions.

Therefore, for the criteria defined in the rest-frame, the RL fraction is 2.0%–4.5% using any single criterion (for R_{uv} considering only the $R_{uv,D}$). This is small compared to the ∼10% seen in typical optically selected AGN samples (e.g. Peterson et al. 1997). To reach 10% would require an additional 22–32 AGNs to be classified as RL. The P_{5GHz} (∼2.0%) is the most restrictive definition of radio-loudness, while R_L (∼4.5%) gives somewhat larger RL samples.

For the criteria defined in the observed frame, we note that no k-correction is included, so for quasars at different redshift, the ratio is actually calculated at a different frequency. The radio loudness definition with radio-to-optical ratio all yield a high radio-loud fraction (> 10%) in contrast to all the other criteria. This is because the quasars in the sample have a large redshift range ($0.1 \leqslant z \leqslant 4.3$). If we consider that most of the quasars in the XMM-COSMOS sample are at redshift 1–2, the rest-frame B band, i band and 5GHz would be at J band, K band and 1.4GHz in the observed frame, then we can define R_J and R_K instead of $R_{L,obs}$ and $R_{i,obs}$, the radio-loud fraction reduce to ∼ 4% and ∼ 2.5% respectively. Although $q_{24,obs}$ also does not include k-correction, it still yields a low radio-loud fraction (2.55%).

Table 3. Radio-Loud Quasar Properties

XID	z	$\log(L_{bol})^*$	$\log(M_{BH}/M_\odot)^{**}$	λ_{Edd}^{***}
40	0.971	45.24	···	···
2282	1.541	45.38	···	···
5230	1.317	46.44	8.21	1.337
5257	1.403	46.07	9.06	0.080
5395	1.472	45.68	···	···
5517	2.132	46.24	8.70	0.277

*$\log(L_{bol})$ is calculated by integrating the rest-frame SED from 1 μm to 40 keV.
** The black hole mass estimates are from Trump et al. (2009b) and Merloni et al. (2010).
***Eddington ratio

$$\lambda_{Edd} = \frac{L_{bol}}{L_{Edd}} = \frac{L_{bol}}{\frac{4\pi G c m_p}{\sigma_e} M_{BH}} = \frac{L_{bol}}{1.26 \times 10^{38} (M_{BH}/M_\odot)}$$

4.2 Pairs of Criteria

We also consider 18 pairs of RL criteria (Table 2). To avoid confusion with k-correction effects, criteria in the observed frame are not compared with criteria in the rest-frame. Thus, these 18 pairs include all the possible combinations of criteria pairs. The RL fraction is determined by the number of objects that lie in the RL-selection region for both measures of radio-loudness divided by the total number of sources in the sample (407; when q_{24} or $q_{24,obs}$ included, it is 382). The "ambiguous" sources include: 1. sources identified as RL by one criterion (detections only) but RQ with the other; 2. sources with only upper/lower limits which lie in the RL region.

If we require any two criteria to agree, then the RL fractions are even smaller (1.5%–4.4%, Table 2) except for $R_{L,obs}$ and $R_{i,obs}$. For about 3/4 of all possible combinations, the RL fraction are smaller or around 2%.

4.3 Solidly Radio Loud Quasars

Finally, if we require all the above criteria to be satisfied simultaneously, just six sources remain[1]. The according RL fraction is thus 1.5% (6 out of 407), only marginally lower than that obtained for a classification with the P_{5GHz} criterion alone. We plot the SEDs of these quasars in Figure 3. The general properties of these quasars are listed in Table 3. For the three of the six, black hole estimates are available and all exceed $10^8 M_\odot$.

4.4 Inter-comparison of Criteria

Figure 4 & 5 show the distributions of the sources with respect to the different RL diagnostics to illustrate the RL fraction and compare the agreement among the above radio loudness definitions. On the side of each axis, we also plot the cumulative fraction of the sources as function of the corresponding radio-loudness measurements using the survival analysis methods (Kaplan & Meier 1958; Schmitt 1985) which we previously employed to compute the RL fractions.

[1] XID=40, 2282, 5230, 5275, 5517, 5395. Note if we use the $R_{uv,D}$ criterion, the quasar XID=5275 is classified as RQ.

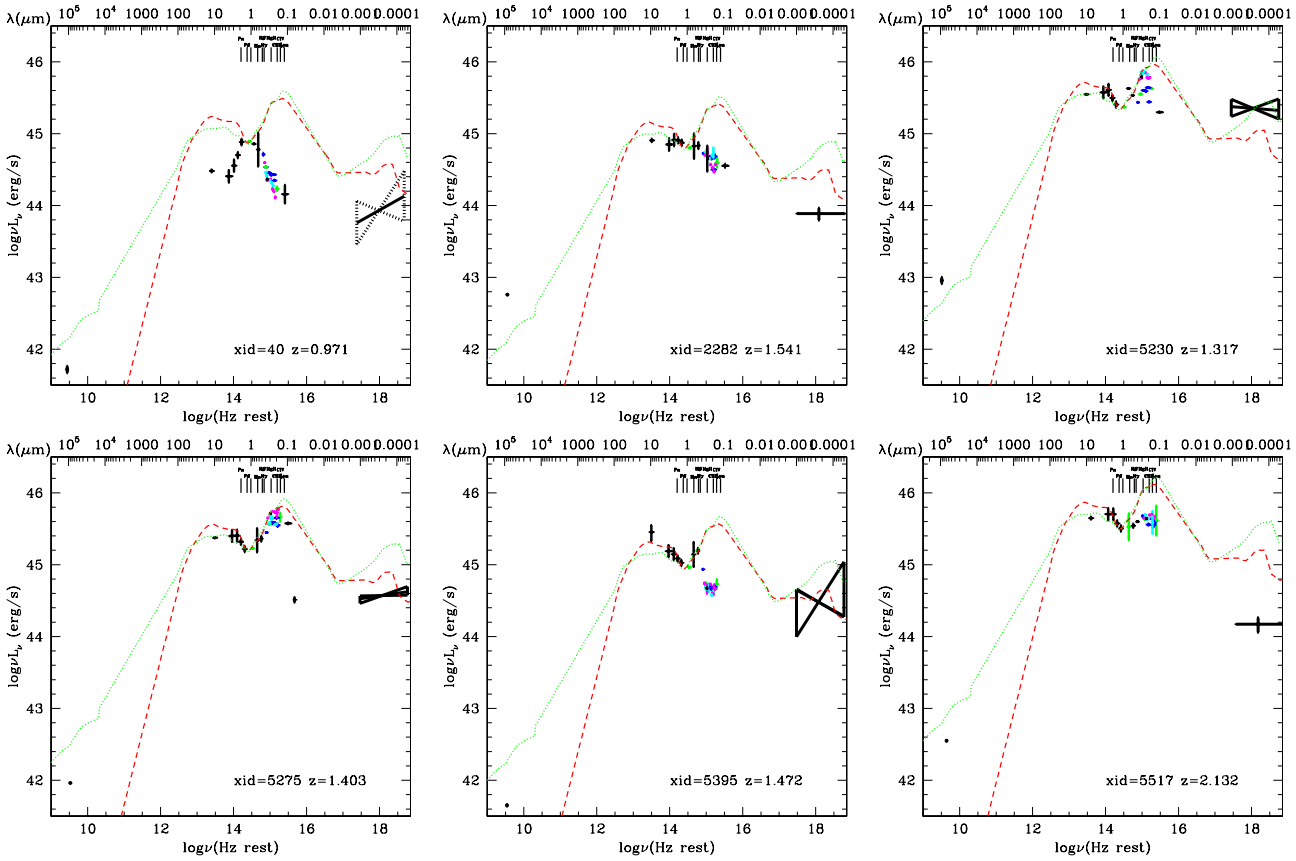

Figure 3. The spectral energy distribution (SED) of the six quasars which are radio-loud in all criteria. The red dashed line is the E94 RQ mean SED. The green dotted line is the E94 RL mean SED. The data points in the SED are color-coded as in Elvis et al. (2012). From low to high frequency, the black data points are: 1.4GHz, 24 μm, 8 μm, 5.7 μm, 4.5 μm, 3.6 μm, K-band, H-band, J-band, NUV, FUV and 2keV. The blue data points are the Subaru broad bands (B_J, g, r, i, z). The green data points are the (CFHT) K-band, and the (CFHT) u band and i band. The purple data points are the 6 Subaru intermediate bands for season 1 (2006) (IA427, IA464, IA505, IA574, IA709, IA827). The cyan data points are the 5 Subaru intermediate bands for season 2 (2007) (IA484, IA527, IA624, IA679, IA738, IA767).

We marked the 6 quasars in the sample that are classified as RL according to all nine criteria with green circles. Their SEDs are plotted in Figure 3.

For the criteria defined in the rest-frame, the radio-loudness defined by the ratios of radio to optical luminosity (R_L, R_{uv} and R_i) correlate well with each other (Figure 4 & 5). The R_X and P_{5GHz} criteria agree the best with the fewest 'ambiguous' quasars.

5 DISCUSSION

5.1 Low Radio-Loud Fraction

We have found a low RL fraction of 1.5%–4.5% (using six different criteria defined in the rest-frame) in the XMM-COSMOS type 1 AGN sample, as compared with about 10% in optically selected samples. For example, in the BQS, Kellermann et al. (1989), find 15% using the R_L criterion; in LBQS, Hooper et al. (1996) find 9% using the rest-frame 8.4 GHz luminosity $\log L_{8.4} > 25$ and 9% using the flux ratio between the rest-frame 8.4 GHz and B band $R_{8.4} > 1$. The difference between XC407 and these other RL fractions is significant at a confidence level of $> 99\%$ and is observed for all RL criteria. In compiling these numbers, we use the criterion $R_{uv,D}$ instead of R_{uv}, as it is subject to reddening and host contamination issues (§4).

Similarly low RL fractions have been reported or inferred in a few other samples, all of which include infrared selection. For example, Richards et al. (2006) reported only 8 RL quasars among a Spitzer-Sloan Digital Sky Survey (SDSS) quasar sample of 259 sources, giving a similarly small RL fraction of 3%, using the criterion of radio luminosity $L_{rad} > 10^{33}\ erg\ s^{-1}\ Hz^{-1}$, that is $\log[L_{rad}(W/Hz)] > 26$, which is stricter than the typical P_{5GHz} criterion we applied in the present analysis.

Donley et al. (2007) found a RL fraction of 3% when they applied the q_{24} criterion to a sample of 62 X-ray selected power-law AGNs in the *Chandra* Deep Field North (CDFN) whose Spitzer IRAC SEDs exhibit the characteristic power-law emission expected for luminous AGNs. Donley et al. (2012) attribute this low RL fraction to the fact that IRAC color-color selection is biased against sources with particularly bright hosts and radio-loud AGN tend to be hosted by bright elliptical galaxies.

Of the criterion defined in the observed frame, the criteria $R_{L,obs}$ and $R_{i,obs}$ yield a high radio-loud fraction

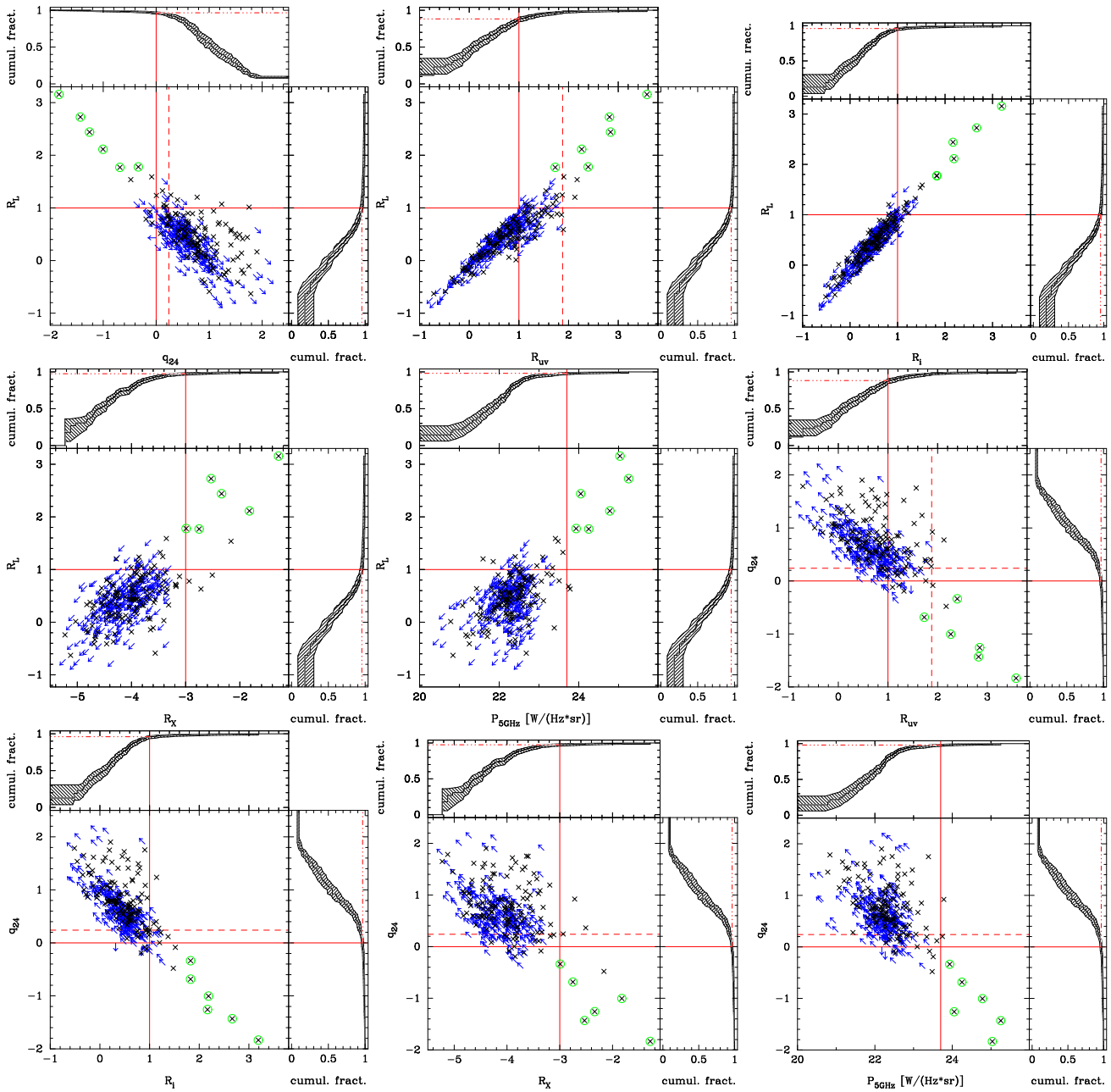

Figure 4. Radio-loudness measures: R_L, q_{24}, R_{uv}, R_i, R_X, and P_{5GHz}. Black crosses = radio detections; blue arrows = upper/lower limits; green circles = RL in all criteria. Solid lines = limits assumed for the radio-loudness definition. Dashed line perpendicular to q_{24} axis = Kuraszkiewicz et al. (in preparation) adjusted q_{24} criterion. Dashed line perpendicular to R_{uv} axis = Della Ceca et al. (1994) adjusted R_{uv} criterion. Along the upper/right-hand edge we show the cumulative distribution functions which include a correction for upper/lower limits. Dash-dotted lines indicate the RQ fraction.

($> 10\%$). This number is comparable to previous studies. For example, in the Sloan Digital Sky Survey –DR2/FIRST, Ivezić et al. (2002) find $8\%\pm1\%$ using the flux ratio between the 1.4 GHz and i band in the observed frame $R_{i,obs} > 1$. However, we note that no k-correction is included in these two criteria and the XMM-COSMOS sample has a large redshift range. Considering most of the quasars in the XMM-COSMOS sample are at redshift 1–2, we define R_J and R_K instead to ensure a more meaningful comparison with the observed frame criteria applied to low redshift samples. The radio-loud fraction then drops to about 4% and 2.5%, respectively. Even though $q_{24,obs}$ also involves no k-correction, the corresponding RL fraction is nevertheless low (2.55%). Therefore, for samples with large redshift range, the criteria defined in the observed frame not including k-correction could give different radio-loud fraction compared to other criteria defined in the rest-frame.

X-ray samples often select more obscured or host dominated AGNs than optically selected samples (Hao et al. 2014, Kuraszkiewicz et al. 2003), because X-ray emission is ubiquitous in AGNs which makes X-ray surveys the most complete census of AGNs of any single band (Risaliti & Elvis

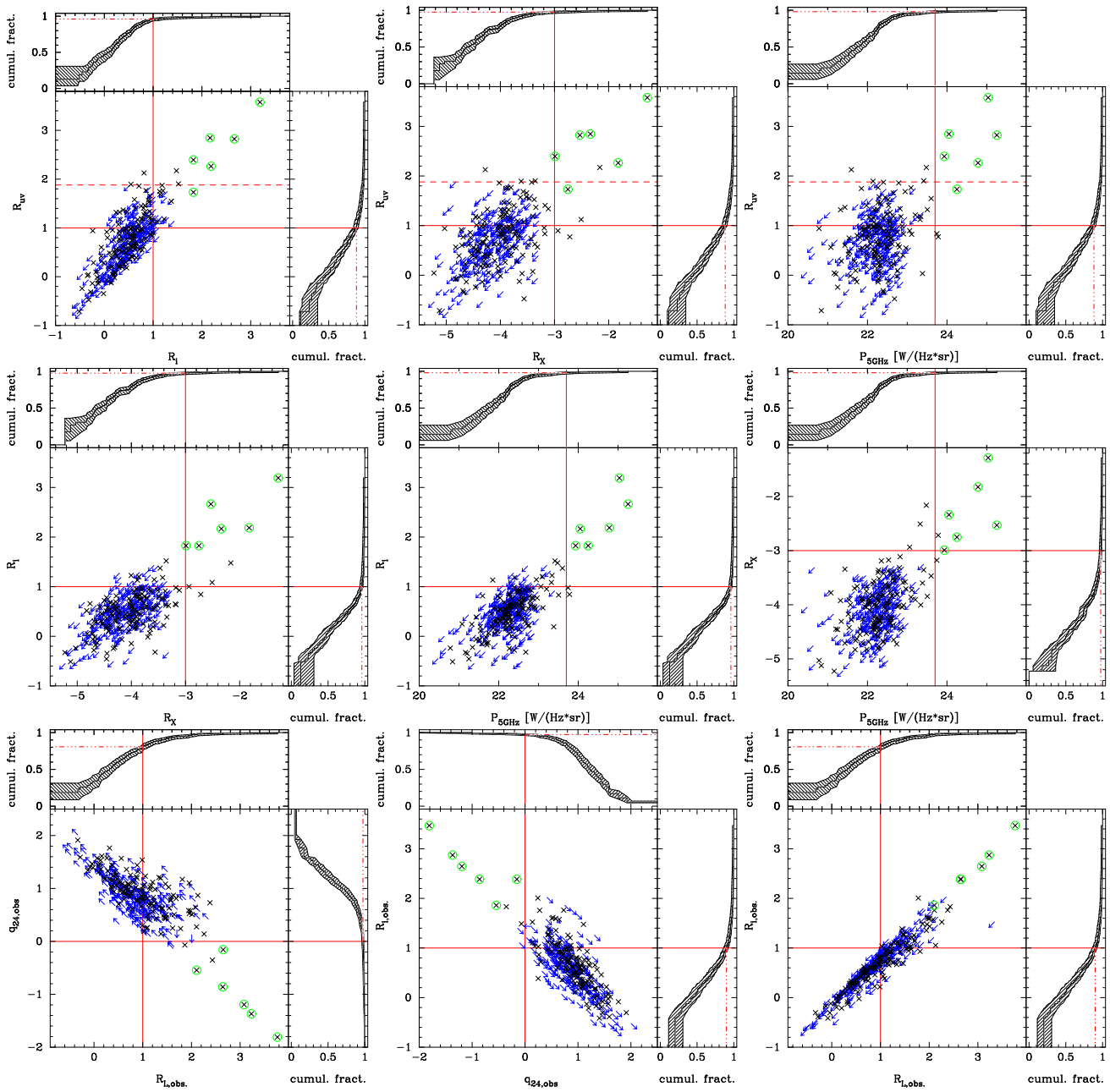

Figure 5. Radio-loudness measures: R_{uv}, R_i, R_X, P_{5GHz}, $R_{L,obs}$, $q_{24,obs}$ and $R_{i,obs}$. Black crosses = radio detections; blue arrows = upper/lower limits; green circles = RL in all criteria. Solid lines = limits assumed for the radio-loudness definition. Dashed line = Della Ceca et al. (1994) adjusted R_{uv} criterion. Along the upper/right-hand edge we show the cumulative distribution functions which include a correction for upper/lower limits. Dash-dotted lines indicate the RQ fraction.

2004). Reddening will increase the RL fraction, as we confirm in the present XMM-COSMOS sample based on the R_{uv} criterion. A large host galaxy contribution could artificially boost the apparent optical flux, thereby fortuitously reducing the RL fraction for most of these criteria (e.g. R_L), while the combination effect of host and reddening still results in higher values of R_{uv}. The host contribution and reddening will effect the criteria defined with an optical luminosity the most. However, both the q_{24} and P_{5GHz} criteria are insensitive to reddening and host contribution, and we find both q_{24} and P_{5GHz} to agree with R_L for this sample (Figure 4). This suggests that neither reddening nor host-contamination are the main reasons for the low RL fraction in this sample.

To ascertain in more detail that reddening and host-contamination do not play a major part in producing the low radio-loud fraction in the XMM-COSMOS sample, we use the mixing diagram (Hao et al. 2013) to estimate the host galaxy fraction at 1 μm (f_g) for each quasar. Here we choose the mixing curve connecting Ell5 (SWIRE galaxy template of elliptical galaxy with age of 5 Gyr, Polletta et al. 2007) and E94 (Elvis et al. 1994 mean quasar SED). As shown in Hao et al. (2013), the difference in galaxy fraction is negligible regardless of the mixing curves cho-

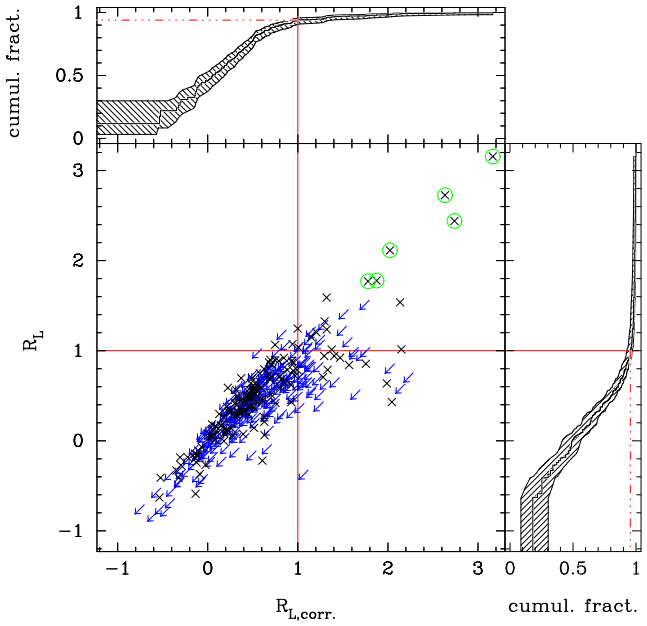

Figure 6. The radio-loudness after correction for the host contribution and reddening ($R_{L,corr}$) compared to the observed radio-loudness (R_L). The plot is color-coded as in Figure 4&5.

sen. The AGN contribution of the luminosity at $1\mu m$ is thus $L_{AGN,1\mu m} = L_{1\mu m}(1 - f_g)$. We assume that the unreddened intrinsic quasar SED has the shape of the E94 SED, which is a reasonable assumption (Hao et al. 2014). We normalize the E94 SED to the pure AGN luminosity at $1\mu m$, and recover the AGN rest-frame B band luminosity from $L_{B,corr} = L_{1\mu m}(1 - f_g) - L_{E94,1\mu m} + L_{E94,B}$. As the radio emission mainly comes from the AGN, the new $R_{L,corr} = \log(L_{5GHz}/L_{B,corr})$ is the radio-loudness corrected for the host galaxy contribution and reddening. Figure 7 shows the comparison between the radio-loudness before and after the correction. The radio-loud fraction for this corrected radio-loudness is $6.08\%^{+3.18\%}_{-1.75\%}$. We can see that it is slightly higher than the radio-loud fraction before the correction, which means the host contribution and reddening in combination decrease the radio-loud fraction. This is consistent with the case of nearby Seyferts (Ho & Peng 2001). However, they are not the most significant factor leading to the low radio-loud fraction found in the XMM-COSMOS sample.

RL quasars usually reside in very massive galaxies and typically have a lower optical or X-ray output at given stellar mass (i.e. lower L/L_{Edd} at given L, Sikora et al. 2007) compared to RQ quasars. This means that a L_X-limited sample will have a lower RL quasar fraction, compared to a mass-limited sample. COSMOS is a deep survey in a limited area, thus it will sample a few high mass ($L > 5L_*$) galaxies at any redshift, compared to wide area shallow surveys (e.g. SDSS), similar to the CDFN sample (Donley et al. 2007) which also has a low radio-loud fraction.

We also note that XC407 is not a complete X-ray selected sample, but a sub-sample with spectroscopic coverage. The optical-near infrared magnitudes of the spectroscopic sub-sample thus tend to be brighter than the complete sample, which in principle produces a bias toward low radio-loudness in the radio-loudness distribution of the complete sample.

5.2 Correlation of Radio-loudness with Other Properties

In the EMSS, Della Ceca et al. (1994) found a 10.6% radio-loud fraction and a trend of lower RL fractions for absolute magnitudes fainter than M_B = - 24. Note that this sample is also X-ray selected but is not restricted to type 1 AGNs. The XMM-COSMOS B band absolute magnitude distribution is similar to that of the EMSS sample (Elvis et al. 2012), with 191 (46% of the whole sample) having $M_B >$ - 24. We plot R_L versus M_B for XC407 in the left panel of Figure 7. Note that we have changed to the same cosmology (H_0 =50 km s^{-1} Mpc^{-1}) as Della Ceca et al. (1994) for M_B. No trend of reduced RL fraction at $M_B < -24$ is seen in our sample.

Radio-loudness is seen to increase with decreasing Eddington ratio (L/L_{Edd}), in particular $R_L \propto (L/L_{Edd})^{-1}$ at $L/L_{Edd} > 0.001$ (Sikora et al. 2007, Ho 2002). However, the XMM-COSMOS sources have relatively high Eddington ratios (> 0.01, with a median of 0.2, Hao et al. 2014). This is similar to the values for PG quasars (Kellerman et al., 1987, Sikora et al. 2007). We plot R_L versus $\log(L/L_{Edd})$ in the middle panel of Figure 7. No trend of reduced RL fraction for large Eddington ratio is visible in our sample. In fact, all the $R_L > 1$ AGNs have $\log(L/L_{Edd}) > -1$.

In E94, the mean SED of the RL and RQ sample show differences in the X-rays (see Figure 3 red and green curve), with RL quasars tending to have relatively brighter X-ray luminosity (about 0.5 dex higher). We checked the R_L versus the X-ray luminosity at 2keV (νL_{2keV}) in the right panel of Figure 7. No obvious trend toward reduced RL fraction at low X-ray luminosity is seen. If we divided the sample at the median νL_{2keV} (43.96 erg/s), slightly more radio loud quasars are above the median, which is 10 radio-loud quasars with radio detections has X-ray luminosity above median compared to 8 radio-loud quasars with radio detections has X-ray luminosity below the median. This is consistent with the mean SED get in E94.

6 SUMMARY

We have used nine different radio-loudness criteria to study the radio loud fraction of the XMM-COSMOS type 1 AGN sample, in which six were defined in the rest-frame (radio loud fraction ranging from 1.5%–4.5%) and three were defined in the observed frame without k-correction. The poor statistics on the RL sources does not allow to infer statistically significant results on a dichotomy between RQ and RL AGN, of which we do not see any sign.

The criteria defined in the rest-frame generally agree with each other and gives similar radio-loud fractions. The criterion R_X and P_{5GHz} agree the best with the smallest number of ambiguous sources. Radio-loudness defined via a radio-to-optical luminosity ratio (R_L, R_{uv} and R_i) display the strongest correlation. The radio power (P_{5GHz}) gives the strongest restriction, that yields the lowest radio-loud fraction for any single criteria. If we require all the criteria to be satisfied at the same time, the radio-loud fraction is

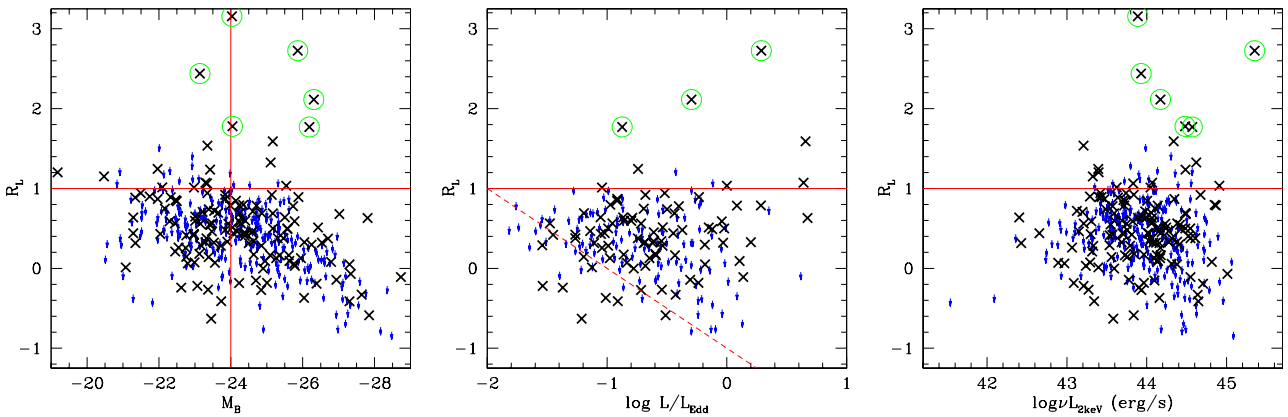

Figure 7. R_L versus M_B (left), $\log(L/L_{Edd})$ (middle) and νL_{2keV} (right) for the XC407 sample, respectively. Here M_B is calculated using H_0 =50 km s^{-1} Mpc^{-1}. The Eddington ratio is $\lambda_{Edd} = L_{bol}/L_{Edd}$. The νL_{2keV} is the 2keV X-ray luminosity in units of erg/s. Note that in the middle plot, we only show 204 among the 407 quasars in the XC407 that have black hole mass estimates (Trump et al. 2009b; Merloni et al. 2010). For the rest of the sample, the broad emission lines are locate at the edge of the spectrum, such that reliable estimates of the black hole mass are not possible (Elvis et al. 2012). The black crosses show the quasars with $> 3\sigma$ detections in the radio and the blue arrows show the quasars with upper limits in the radio. The green circles indicate the 6 sources classified as RL by all criteria. The red dashed line in the center panel shows $R_L = -\log(L/L_{Edd}) - 1$ which represents the general trend found in Sikora et al. (2007).

marginally smaller than the radio-loud fraction we get from the P_{5GHz} criterion only.

Two of the criteria defined in the observed frame without k-correction give a much higher radio-loud fraction, but if we take the redshift distribution of the sample into consideration, the radio-loud fraction is greatly reduced and becomes consistent with the results from the criteria defined in the rest-frame. Thus, we need to be careful when citing the radio-loud fraction using the criteria defined in the observed frame without k-correction.

If we corrected the host galaxy contribution and reddening, the radio-loud fraction in the XC407 sample will rise to $6.08\%^{+3.18\%}_{-1.75\%}$, still a bit smaller than the typical value of 10% in optical selected samples, which might be caused by the selection of the sample being L_X-limited and biasing towards bright optical quasars. No correlation of the radio-loudness with M_B, L/L_{Edd} or L_X is seen in the XC407 sample.

The combination of newly approved deep 3GHz EVLA observations (P.I.: Smolcic) with the completion of Chandra coverage of the whole COSMOS field in the COSMOS Legacy survey (P.I.: Civano) will help us understand the origin of the low RL fraction of type 1 AGNs.

ACKNOWLEDGMENTS

HH thank Belinda Wilkes for useful discussion. This work was supported in part by NASA *Chandra* grant number G07-8136A (HH, ME, CV). LCH acknowledges support from the Kavli Foundation, Peking University, and the Chinese Academy of Science through grant No. XDB09030100 (Emergence of Cosmological Structures) from the Strategic Priority Research Program. Support from the Italian Space Agency (ASI) under the contracts ASI-INAF I/088/06/0 and I/009/10/0 is acknowledged (AC and CV). MS acknowledges support by the German Deutsche Forschungsgemeinschaft, DFG Leibniz Prize (FKZ HA 1850/28-1). KS gratefully acknowledges support from Swiss National Science Foundation Grant PP00P2_138979/1.

REFERENCES

Appleton, P. N., et al., 2004, ApJS, 154, 147
Baloković, M., Smolčić, V., Ivezić, Ž., Zamorani, G., Schinnerer, E., and Kelly, B. C., ApJ, 2012, 759, 30
Brusa, M., et al., 2005, A&A, 2005, 421, 69
Brusa, M., et al., 2007, ApJS, 2007, 172, 353
Brusa, M., et al., 2010, ApJ, 716, 348
Capak, P., et al., 2007, ApJS, 172, 99
Capak, P., et al., 2010, in preparation
Cirasuolo, M., et al., 2007, MNRAS, 380, 585
Cirasuolo, M., et al., 2003, MNRAS, 341, 993
Della Ceca, R., Zamorani, G., Maccacaro, T., Wolter, A., Griffiths, R., Stocke, J. T., & Setti, G., 1994, ApJ, 430, 533
Donley, J. L., Rieke, G. H., Pérez-González, P. G., Rigby, J. R., Alonso-Herrero, A., 2007, ApJ, 660, 167
Donley, J. L., et al., 2012, ApJ, 748, 142
Elvis, M. et al., 1994, ApJS, 95, 1
Elvis, M. et al., 2012, ApJ, 759, 6
Feigelson, E. D. & Nelson, P. I., 1985, ApJ, 293, 192
Goldschmidt, P., Kukula, M. J., Miller, L., & Dunlop, J. S., 1999, ApJ, 511, 612
Hao, H. et al. 2014, MNRAS, 438, 1288
Hao, H. et al. 2013, MNRAS, 434, 3104
Harris, D. E., & Krawczynski, H., 2006, ARA&A, 44, 463
Hasinger, G., et al., 2007, ApJS, 172, 29
Ho, L. C., 2002, ApJ, 564, 120
Ho, L. C., & Peng, C. Y., 2001, ApJ, 555, 650
Hooper, E. J., et al., 1996, ApJ, 473, 746
Ivezić, Ž., 2004, in Multiwavelength AGN Surveys, ed. R.Mújica & R. Maiolino (Singapore: World Scientific), 53
Ivezić, Ž., et al., 2002, AJ, 124, 2364

Jiang, L., Fan, X., Ivezić,Ž., Richards, G. T., Schneider, D. P., Strauss, M. A., & Kelly, B. C., 2007, ApJ, 656, 680
Kaplan, E. L., & Meier, P. 1958, J. Am. Statistical Association, 53, 457
Kellermann, K. I., et al., 1989, AJ, 98, 1195
Komatsu, E., et al., 2009, ApJS, 180, 330
Kuraszkiewicz, J. K., et al. 2003, ApJ, 590, 128
Le Floc'h, E. et al., 2009, ApJ, 703, 222L
Lilly, S. J., et al., 2007, ApJS 172, 70
Lilly, S. J., et al., 2009, ApJS 184, 218
Merloni, A., et al. 2010, ApJ 708, 137
Miller, R. G., Jr. 1981, Survival Analysis (New York; Wiley)
Miller, L., et al., 1990, MNRAS, 244, 207
Peterson, B. M. 1997, An Introduction to Active Galactic Nuclei (Cambridge: Cambridge University Press)
Pierce, C. M., Ballantyne, D. R., & Ivison, R. J., 2011, ApJ, 742, 45
Polletta, M. et al. 2007, ApJ, 663, 81
Richards, G. T., et al., 2006, ApJ, 166, 470
Risaliti, G. & Elvis, M., 2004, in ASSL Vol 308, Supermassive Black Holes in the Distant Universe, ed. A. J. Barger (Dordrecht: Kluwer), 187
Sargent, M. T., et al. 2010, ApJS, 186, 341
Schinnerer, E., et al., 2007, ApJS, 172, 46
Schinnerer, E., et al., 2010, ApJS, 188, 384.
Schmitt, J. H. M. M. 1985, ApJ, 293, 178
Scoville, N. Z., et al., 2007, ApJS, 172, 1
Scoville, N. Z., et al., 2007, ApJS, 172, 38
Sikora, M., Stawarz, L. & Lasota, J. P., 2007, ApJ, 658, 815
Spergel, D. N., et al., 2007, ApJS, 170,377
Stocke, J. T., Morris, S. L., Weymann, R. J. & Foltz, C. B., 1992, ApJ, 396, 487
Terashima, Y. & Wilson, A. S. 2003, ApJ, 583, 145
Trump, J. R., et al., 2007, ApJS, 172, 383
Trump, J. R., et al., 2009a ApJ, 696, 1195
Trump, J. R., et al., 2009b ApJ, 700, 49
Urry, C. M. & Padovani, P., 1995, PASP, 107, 803
Visnovsky, K. L., et al., 1992, ApJ, 391, 560
Wilkes, B. J. & Elvis, M., 1987, ApJ, 323, 243
Zamorani, G., et al., 1981, ApJ, 245, 357